

Article

Histopathologic Findings in the Areas of Orange Pigment Overlying Choroidal Melanomas

Maria D. Garcia¹, Diva R. Salomao², Alan D. Marmorstein³, and Jose S. Pulido^{4,5}

¹ Department of Mayo Medical School, Mayo Clinic, Rochester, MN, USA

² Department of Anatomic Pathology, Mayo Clinic, Rochester, MN, USA

³ Department of Ophthalmology Research, Mayo Clinic, Rochester, MN, USA

⁴ Department of Ophthalmology, Mayo Clinic, Rochester, MN, USA

⁵ Department of Molecular Medicine, Mayo Clinic, Rochester, MN, USA

Correspondence: Jose S Pulido, Mayo Clinic, Department of Ophthalmology and Department of Molecular Medicine, 200 First Street, SW, Rochester, MN 55905, USA. e-mail: pulido.jose@mayo.edu

Received: 04 November 2015

Accepted: 06 February 2016

Published: 12 May 2016

Keywords: choroidal melanoma; uveal melanoma; orange pigment; retinal pigment epithelium; lipofuscin; melanolipofuscin; melanin

Citation: Garcia MD, Salomao DR, Marmorstein AD, Pulido JS. Histopathologic findings in the areas of orange pigment overlying choroidal melanomas. *Trans Vis Sci Tech.* 2016; 5(3):4, doi:10.1167/tvst.5.3.4

Purpose: Orange pigment is an important sign of malignancy in melanocytic tumors. There is a question as to whether the pigment accumulation is inside of macrophages or retinal pigment epithelial (RPE) cells. We investigated which cells are involved with this color alteration.

Methods: We examined enucleated specimens from two patients with choroidal melanoma and dense orange pigment on fundus examination. Color fundus and fundus autofluorescence (FAF) photographs were reviewed followed by examination with fluorescent microscopy, electron microscopy, and immunohistochemistry of enucleated eyes for the specific areas corresponding to the orange pigment.

Results: Orange pigment was observed on color fundus photography and correlated with areas of hyperautofluorescence on FAF. Fluorescent microscopy of sections of the enucleated eyes showed autofluorescence in the RPE, which were most pronounced where there was a localized retinal detachment and reactive hyperplasia of the RPE. Immunohistochemical studies were done with keratin (OSCAR and AE1/AE3) and S-100 stained RPE cells, which still were attached to Bruch's membrane. Histiocytes present in the detached retina stained with anti-CD163 antibody and did not show autofluorescence. Electron microscopy studies of the same areas showed the presence of lipofuscin and melanolipofuscin within the clustered RPE cells.

Conclusions: Orange pigment in choroidal melanocytic lesions originates from the RPE cells, rather than macrophages, and is most abundant where there is proliferation of the RPE.

Translational Relevance: The orange pigment tumoral biomarker arises and is in the retinal pigment epithelium.

Introduction

The most common primary intraocular tumor is a choroidal melanoma, and patients who suffer this type of neoplasm have an approximately 50% mortality rate over the next 10 years.¹ Although it has been observed clinically that orange pigment overlying choroidal melanocytic lesions is an important sign of malignant choroidal melanomas, the cells that produce the orange pigment are unknown.²

Orange pigment has been previously shown by one of the authors (JSP) to be autofluorescent.³ Others have confirmed this finding.⁴⁻⁶ Lipofuscin is a pathologic term used to describe yellow-brown

pigment granules that can accumulate in a cell with age or disease. In retinal pigment epithelial (RPE) cells, age-related lipofuscin granules contain lipids, proteins, and retinoid derivatives, including N-retinyl-N-retinylidene ethanolamine.⁷ It is hypothesized that lipofuscin is a byproduct of the oxidative breakdown of the outer segment of photoreceptors in the retina and that retinoid derivatives are the principal contributors to lipofuscin autofluorescence.⁸⁻¹¹ Furthermore, lipofuscin accumulation suggests abnormal lysosomal mechanisms leading to inadequate breakdown of retinal molecules. Lipofuscin accumulation correlates with a number of ocular diseases, such as age-related macular degeneration; though, with the exception of Stargardt's disease and ceroid lipofus-

Table 1. Primary Antibodies Used in the Immunohistochemical Studies

Antibody	Dilution	Source (Clone)
Keratin AE1/AE3	1/200	Dako (AE1&AE3)
Keratin OSCAR	1/100	Covance (OSCAR)
Keratin CAM5.2	1/50	BD Bioscience (Cam 5.2)
Keratin 7	1/200	Dako (OV-TL12/30)
CD163	1/200	Leica (Novocastra) (10D6)
S100	1/4000	Dako (Polyclonal)
SmooMA	1/3000	Dako (1A4)
Vimentin	1/500	Dako (V9)

cinosis, the significance of lipofuscin accumulation as driving the pathology of the disease state or as an indicator of prognosis is questionable.^{12–17}

Despite the appearance of orange pigment overlying choroidal melanomas, our knowledge of the cellular and subcellular localization of this orange pigment is limited.^{6,18,19} As a result, it is difficult to assess how orange pigment may contribute to the etiology of choroidal melanoma and the degeneration of adjacent retinal tissues. To better understand the association of orange pigment with retinal degeneration in patients with choroidal melanoma, we determined the location of the orange pigment in enucleated eyes from patients with choroidal melanomas. Our data indicated that orange pigment associated with choroidal melanoma is localized to lipofuscin and melanolipofuscin granules in RPE cells overlying the tumor.

Methods

After obtaining approval from the Mayo Clinic Institutional Review Board, we reviewed the records of two patients with choroidal melanomas who had enucleations at Mayo Clinic in Rochester, MN. Our study complied with the Declaration of Helsinki.

Both patients had a complete ocular examination, which included Snellen visual acuity, slit-lamp biomicroscopy, intraocular pressure, and funduscopy. Furthermore, optical coherence tomography (OCT), color fundus photographs, and autofluorescence photographs also were obtained. Fundus autofluorescence (FAF) photographs were attained with the Heidelberg confocal scanning laser ophthalmoscope system (Heidelberg Retina Angiograph [HRA]; Hei-

delberg Engineering, Dossenheim, Germany). In this machine, autofluorescence is excited by using argon blue wavelength (488 nm). We examined the color fundus and autofluorescence photographs for the presence of orange pigment and autofluorescence, respectively.

The enucleated eyes were fixed for a minimum of 48 hours in buffered formalin at 10%. Following fixation, these eyes were examined, photographed, and sectioned following guidelines for examination of enucleated eyes with uveal melanoma.²⁰ Sections of the eyes were paraffin-embedded and submitted to histologic preparation and staining with hematoxylin-eosin (H&E) and periodic acid–Schiff (PAS) for subsequent microscopic examination.

Additional sections were examined from areas identified as orange pigment–rich by comparison with the autofluorescence photographs. Using fluorescent microscopy, a few unstained sections were evaluated for the location of areas with higher concentration of autofluorescent lipofuscin. Selected tissue sections were stained with immunohistochemistry (Table 1). Antibodies against CD68 and CD163 were used to identify macrophages. Antibodies against S-100 and cytokeratins: keratin 7, CAM 5.2 (keratins 7 and 8), AE1/AE3 (keratins 1–8, 10, 14–16, and 19), and OSCAR Keratin (pan-keratin cocktail) were used to immunophenotype the RPE cells.

Unstained tissue sections with higher concentration of autofluorescent lipofuscin were selected and marked to be evaluated by electron microscopy; 10- μ m paraffin-embedded tissue sections were placed onto glass slides. The unstained sections were deparaffinized by placing the slide into warm xylene for 60 minutes. The slide then was transferred to absolute ethanol at 60°C for 30 minutes followed by a decreasing concentration of ethanol to 60%. The slide then was fixed in Trump's fixative (1% glutaraldehyde and 4% formaldehyde in 0.1 M phosphate buffer, pH 7.2) overnight.²¹ The slide then was rinsed for 30 minutes in three changes of 0.1 M phosphate buffer, pH 7.2, followed by a 1-hour postfix in phosphate-buffered 1% osmium tetroxide (OsO₄). After rinsing in three changes of distilled water for 30 minutes, the tissue was en bloc stained with 2% uranyl acetate for 30 minutes at 60°C. After en bloc staining, the tissue was rinsed in three changes of distilled water, dehydrated in progressive concentrations of ethanol and 100% propylene oxide, and embedded in Spurr's resin.²² Thin (90 nm) sections were cut on a Leica UC6 ultramicrotome (Leica, Wetzlar, Germany), placed on 200 mesh copper grids, and stained with



Figure 1. Color fundus photographs (a, c) and FAF photographs (b, d) of a diffuse choroidal melanoma. Images (a, b) are from the right eye of patient 1. The tumor is located inferotemporally with arrows showing the presence of orange pigment on image (a). Arrows in the FAF image (b) demonstrate increased autofluorescence, which correlates with the location of the orange pigment observed with color fundus photography. Images (c, d) are from the left eye of patient 2. The tumor is located superotemporally. Arrows point to orange pigment (c) and increased autofluorescence (d), with similar findings to those seen in images (a) and (b), respectively.

lead citrate. Micrographs were taken on a JEOL 1400 plus transmission electron microscope (JEOL USA, Inc., Waterford, VA) operating at 80 KV.

Results

Two patients, who elected to have enucleation for their choroidal melanomas, were included in this study. Patient 1 is a 50-year-old-man with a diffuse infiltrative posterior choroidal melanoma located inferotemporally on the right eye. Color fundus photography showed an area of orange pigmentation (Fig. 1a). Furthermore, FAF imaging demonstrated the autofluorescent nature of this pigment, suggesting the presence of lipofuscin (Fig. 1b).

Patient 2 was a 58-year-old-man with a diffuse posterior choroidal melanoma located superotemporally on the left eye. Color fundus photography and FAF showed orange pigment and autofluorescence, respectively (Figs. 1c, 1d).

Upon examining enucleated specimens from both patients, using fluorescent microscopy, autofluorescence was present along the RPE with areas of intensified fluorescence corresponding to RPE cells stacking over each other (Figs. 2b, 2c). We observed the presence of lipofuscin in cells that were attached, as well as detached from Bruch's membrane (BM). In areas where the RPE is attached, autofluorescence can be seen outlining the location of the RPE (Fig. 2a). However, the autofluorescence is most prominent inside RPE cells that are hyperplastic and stacking up in areas of localized retinal detachment (Figs. 2b, 2c). The autofluorescence appeared to be emanating from granules in the RPE.

Using H&E stained sections, we observed RPE cells stacking up and undergoing reactive changes (Fig. 3). Furthermore, H&E stains demonstrated that macrophages were only present free floating in the subretinal fluid in areas where the retina was detached from BM (Fig. 3a). Sections stained with PAS revealed similar results, with spindle-shaped RPE cells stacking to form a multi-layered RPE along areas of detachment (Figs. 4a, 4c). Immunohistochemistry showed that the spindle-shaped cells were not macrophages (Fig. 4e).

These same tissue sections also were analyzed using immunohistochemistry. The results for the immunostains are summarized in Tables 2 and 3. Anti-CD163 antibodies showed strong immunorexpression in macrophages within the tumor mass, while anti-CD68 antibodies only mildly stained these cells (Table 2). Both antibodies stained free-floating macrophages in the areas of retinal detachment overlying the tumor mass. PAS stain helped to highlight BM (Fig. 4c). Retinal pigment epithelial cells consistently stained positive for OSCAR Keratin, AE1/AE3, and S-100 in areas where these cells were attached to BM (Table 2). Although there also was some degree of immunorexpression along the RPE for CAM 5.2 and keratin 7, this was present only in some focal areas where the RPE cells appeared spindle-shaped; this was consistent with reactive changes associated with the underlying tumor mass effect and areas of detachment (Table 2). These spindle-shaped cells did not react with antibodies directed against smooth muscle actin (SMA) but did have some degree of positivity for vimentin (Tables 2 and 3).

Keratin OSCAR stained these RPE cells undergoing reactive changes (Figs. 4b, 4d, 4e). Antibodies against CD163 confirmed the presence of histiocytes in the subretinal fluid and allowed us to distinguish

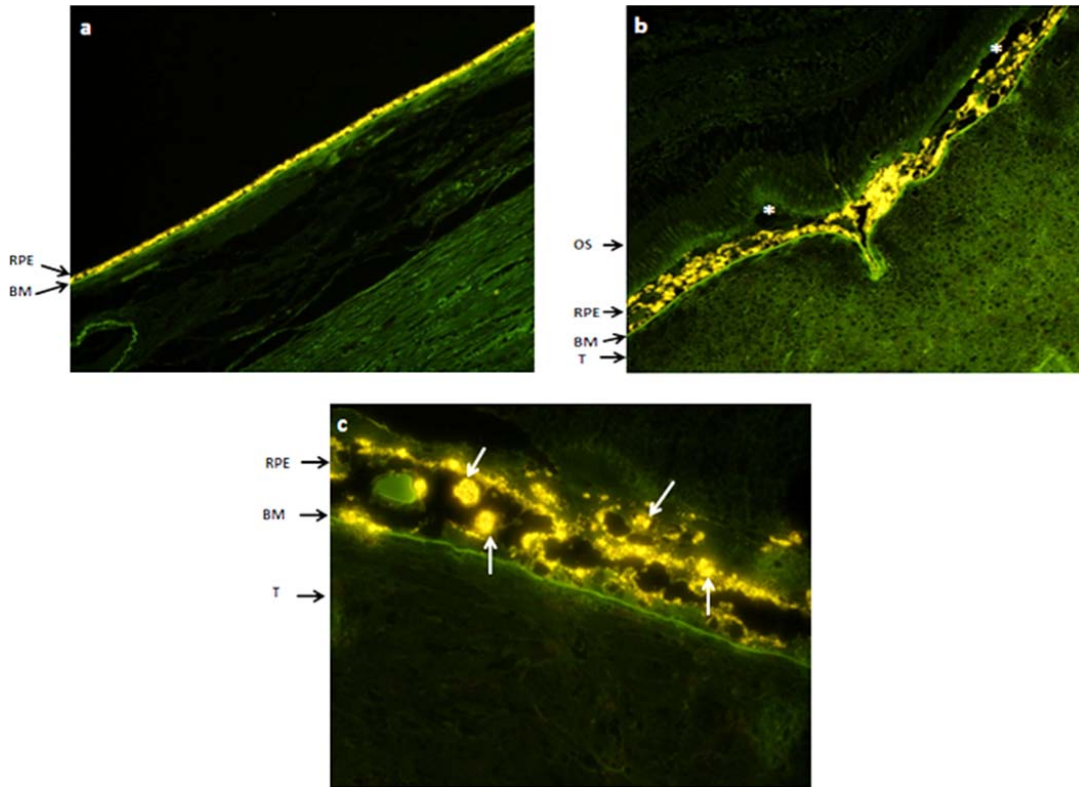


Figure 2. Immunofluorescent images from the enucleated left eye with a choroidal melanoma from patient 2. The RPE appears yellow due to the autofluorescent nature of lipofuscin. Image (a) shows a tumor-free area; the RPE has a normal linear pattern with attachment to BM; original magnification $\times 20$. In contrast, image (b) demonstrates the proliferation of the RPE where the tissue is infiltrated by tumor cells. The white asterisks represent detachment from BM; original magnification $\times 20$. OS, outer segments of photoreceptors; T, tumor cells. Image (c) is a magnified ($\times 40$) view of the choroidal melanoma showing yellow autofluorescent globules of lipofuscin (white arrows) inside the reactive RPE.

these cells from the RPE cells (Fig. 4f). Furthermore, electron microscopy studies of the same areas showed the presence of clusters of RPE cells actually containing lipofuscin and melanolipofuscin pigment (Fig. 5).

Discussion

In this study, we found that the striking orange pigment overlying choroidal melanomas originates

from proliferating RPE cells containing intracellular lipofuscin and melanolipofuscin granules. Previous studies have associated the orange pigment produced with macrophages and RPE cells.^{6,11,18,19,23} We used color fundus photography, FAF, immunohistochemistry, fluorescent microscopy, and electron microscopy to determine which cells are responsible for producing this pigment. Due to the fluorescent nature of the pigment, we were able to clearly visualize its exact location. When we examined

Table 2. Immunostain Results for RPE Overlying Choroidal Melanoma

Patient	Eye	Keratin OSCAR	Keratin CAM5.2	Keratin AE1/AE3	Keratin 7	CD68
#1	OD	+ Cellular membrane	Focal + Basal membrane	+ Cellular membrane	NA	NA
#2	OS	+ Spindling cells in clustered areas	Focal + Spindle cell	Focal + Spindle cell	+ Spindling cells in clustered areas	+ Mildly stained

Table 2. Continued

Patient	CD163	S100	SMA	Vimentin
#1	+ Macrophages floating in detached retina	+ Nuclear staining	-	+
#2	+ Macrophages floating in detached retina	+ Nuclear staining	-	Focal + in the clustered areas

enucleated specimens, autofluorescent globules of lipofuscin were observed all along the RPE. This was most pronounced in areas where the RPE was detached from BM. These areas of detachment

showed proliferation of the RPE cells, with clumping of these cells and abundant autofluorescent globules of lipofuscin. This proliferation of the RPE along the area of the tumor has been reported previously in the

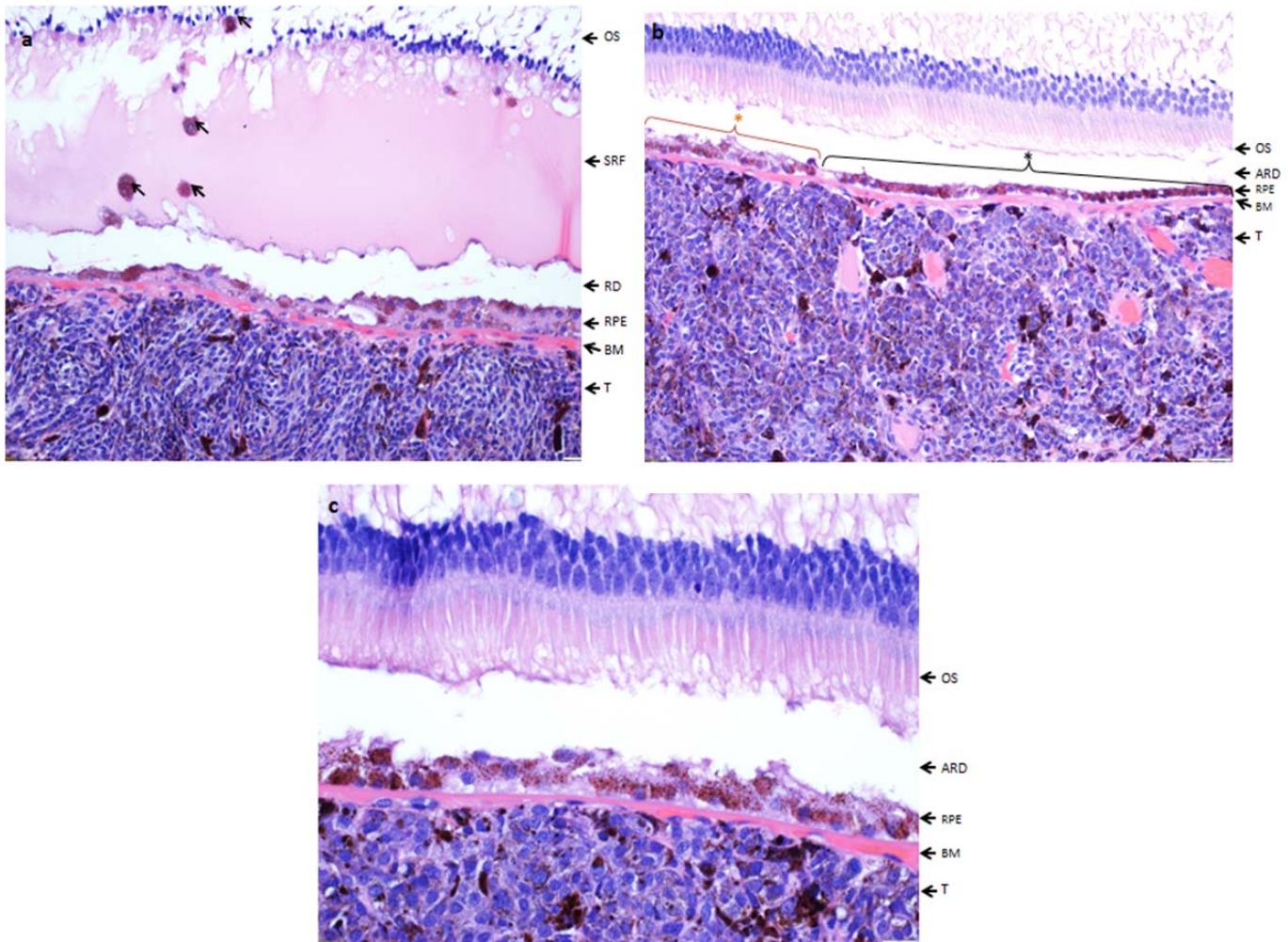


Figure 3. Right eye from patient 1. H&E stains show the RPE overlying a choroidal melanoma. Image (a) specifically shows an area of retinal detachment (RD) with RPE-reactive changes and histiocytes (*black arrows*); original magnification $\times 200$. The *left side* of image (b) shows artifactual retinal detachment (ARD) with RPE-reactive changes (*red asterisk*). In comparison, the *right side* shows a normal layer of RPE cells (*black asterisk*); original magnification $\times 200$. Image (c) shows the reactive changes that the RPE has undergone at $\times 400$ original magnification; OS, outer segments of photoreceptors; SRF, subretinal fluid; T, tumor cells.

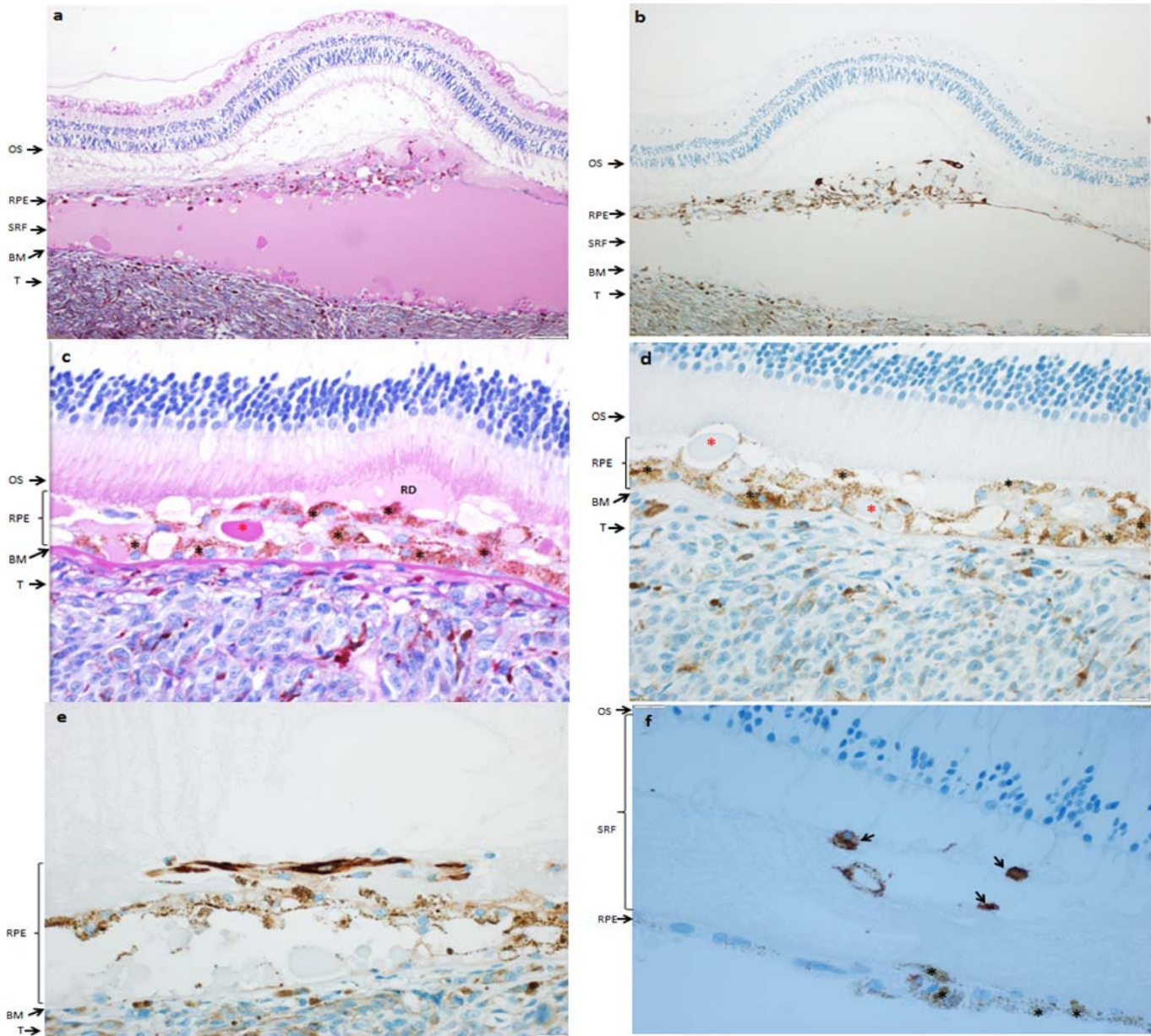


Figure 4. Left eye from patient 2. Image (a) is a PAS stain of a section of the tumor mass. There is retinal detachment with SRF collection. Furthermore, reactive changes can be seen in the RPE characterized by the cells piling up and spindling; original magnification $\times 100$. Image (b) shows the same section as image (a) stained with Keratin OSCAR. The RPE cells stain positive; original magnification $\times 100$. Images (c, d) are magnified ($\times 400$) sections stained with PAS and OSCAR Keratin, respectively. The reactive changes of the RPE are observed here as well. *Black asterisks* highlight the granules of lipofuscin contained within the RPE cells. The *red asterisks* represent drusen. Image (c) demonstrates an area of early RD. The spindle-like phenotype of the RPE cells can be clearly visualized on image (e); original magnification $\times 400$. Image (f) was obtained through immunohistochemistry using anti-CD163 antibodies. There is strong immunorepression for macrophages (*black arrows*), which are seen floating in subretinal fluid. In comparison, *golden brown* lipofuscin granules are present inside of reactive-RPE cells (*black asterisks*); original magnification $\times 400$.

literature.²⁴ We believe that this proliferation of RPE cells overlying the tumor mass directly correlates with the orange pigmentation seen on fundus photography. Thus, as RPE cells filled with granules of lipofuscin proliferate and clump along the tumor,

areas of orange pigmentation become more pronounced.

Although macrophages also have been associated with lipofuscin, we rarely observed fluorescent histiocytes under the fluorescent microscope.²⁵ Others

Table 3. Immunostain Results for RPE on Opposite Side of the Tumor

Patient	Eye	Keratin OSCAR	Keratin CAM5.2	Keratin AE1/AE3	Keratin 7	CD68	CD163
#1	OD	+ Cellular membrane	Focal + Basal membrane	+ Cellular membrane	NA	NA	-
#2	OS	+ Cellular membrane	- Overall, with focal basal membrane	- Overall, with focal basal membrane	-	-	-

have postulated that abnormalities along BM draws macrophages.²⁴ This may be the reason why others have observed macrophages along the tumor and not because these cells are directly responsible for the production of lipofuscin and its orange pigment. Furthermore, other studies have recognized that a commonly used macrophage marker, CD68, can be also present on the surface of RPE cells.^{23,26} Thus, if this marker were used alone, the autofluorescent lipofuscin would have been thought to be associated with macrophages.

Upon examining the RPE cells with immunohistochemistry, we confirmed with a CD163 stain that macrophages were sparse in the areas where lipofuscin was located. Specifically, macrophages were only observed floating in fluid around the areas of retinal detachment. In comparison, RPE cells attached to BM stained with OSCAR Keratin, AE1/AE3, and S-100, and confirmed that it is the RPE cells that are harboring the autofluorescent globules observed under fluorescent microscopy. The RPE cells at sites

of detachment did not stain for any of the epithelial markers mentioned above. This is likely due to the fact that these RPE cells were undergoing reactive changes, resulting in some modification of their phenotype that might resemble mesenchymal cells. These changes have been described by Damato and Foulds²⁴ and called “tumor-associated retinal pigment epitheliopathy.” We observed that the monomorphic cuboidal appearance of the monolayer of RPE cells attached to BM is transformed into spindle-shaped RPE cells that stack up forming a multilayer of cells in areas where the RPE detaches. Our study confirms their findings that RPE cells undergo metaplasia into a phenotype that resembles fibroblasts.²⁴

A limitation of this study stems from the fact that there is a lack of data on what stains are most reliable for the identification of macrophages and RPE cells. One of the most extensive studies on the detection of RPE cells found that the monoclonal antibody CAM 5.2 against cytokeratin 7 and 8, as

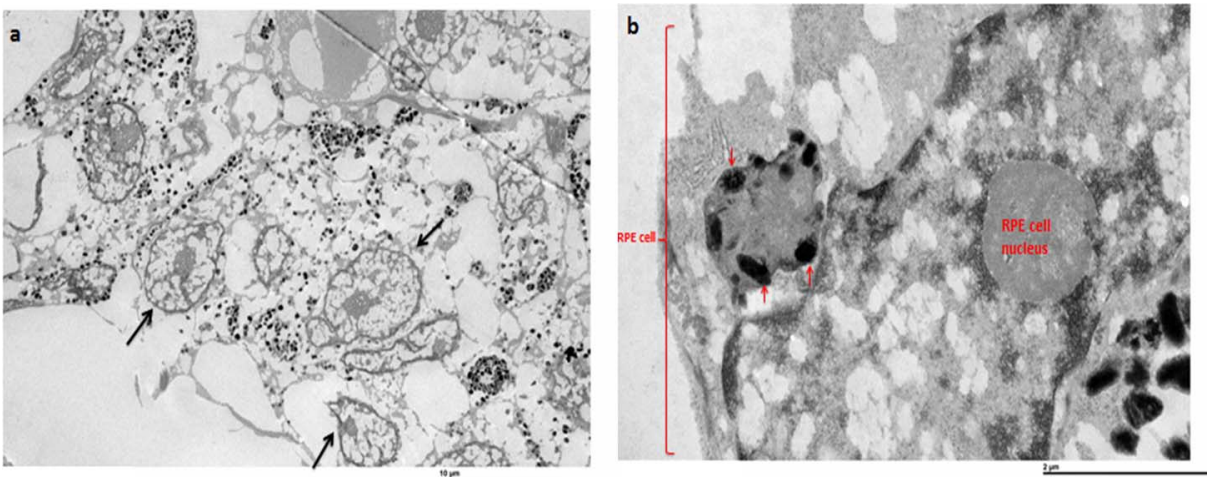


Figure 5. Electron microscopy of RPE cells. Image (a) from patient 1 demonstrates a cluster of RPE cells (*black arrows*) with numerous melanosomes. Both melanin (*black granules*) and lipofuscin (*gray granules*) can be visualized around the RPE cells. Image (b) from patient 2 shows an RPE cell with melanolipofuscin granules (*red arrows*).

Table 3. Extended.

Patient	S100	SMA	Vimentin
#1	+ Nuclear staining	-	+
#2	+ Nuclear staining	-	-

well as antibodies against cytokeratin 18 and 19, strongly labeled RPE cells.²⁷ However, when we examined our tissue sections with CAM 5.2 and cytokeratin 7 antibodies, RPE cells stained inconsistently. As previously mentioned, there also is debate as to what stains are most reliable for the detection of macrophages, as it has been reported in the literature that anti-CD68 antibody, which is used commonly to identify macrophages, also can detect RPE cells.²⁶ Immunostudies might show different results across different laboratories where diverse clones of antibodies are used and due to differences in antigen retrieval techniques. Despite this limitation, we are confident that the orange pigment is originating from the proliferating RPE cells, as our findings from immunohistochemistry were consistent with what we observed under the fluorescent microscope. In addition, whether the autofluorescent orange pigment is from lipofuscin granules or from melanolipofuscin granules, or from both within the RPE cells cannot be determined from this study.

In summary, our data show that the orange pigment overlying choroidal melanocytic lesions originates from RPE cells rather than macrophages. In addition, lipofuscin and/or melanolipofuscin and the corresponding autofluorescence are most prominent where there is proliferation of the RPE cells overlying the tumor mass and at sites of detachment from BM. These areas correspond to where orange pigment is visualized best in the fundus examination of the patients in our study.

Acknowledgments

Supported in part by unrestricted grants from Research to Prevent Blindness, Inc., from the Paul Family, and the Deshong Family.

Disclosure: **M.D. Garcia**, None; **D.R. Salomao**, None; **A.D. Marmorstein**, None; **J.S. Pulido**, None

References

1. Seddon JM, Moy CC. Choroidal melanoma: prognosis. In: Ryan, SR, ed. *Retina*, 3rd ed. St. Louis: CV Mosby; 2001;687–699.
2. Amselem L, Pulido JS, Gunduz K, et al. Changes in fundus autofluorescence of choroidal melanomas following treatment. *Eye (Lond)*. 2009;23:428–434.
3. Gunduz K, Pulido JS, Bakri SJ, Petit-Fond E. Fundus autofluorescence in choroidal melanocytic lesions. *Retina*. 2007;27:681–687.
4. Almeida A, Kaliki S, Shields CL. Autofluorescence of intraocular tumours. *Curr Opin Ophthalmol*. 2013;24:222–232.
5. Materin MA, Raducu R, Bianciotto C, Shields CL. Fundus autofluorescence and optical coherence tomography findings in choroidal melanocytic lesions. *Middle East Afr J Ophthalmol*. 2010;17:201–206.
6. Shields JA, Rodrigues MM, Sarin LK, Tasman WS, Annesley WH Jr. Lipofuscin pigment over benign and malignant choroidal tumors. *Trans Sect Ophthalmol Am Acad Ophthalmol Otolaryngol*. 1976;81:871–881.
7. Gunduz K, Pulido JS, Ezzat K, Salomao D, Hann C. Review of fundus autofluorescence in choroidal melanocytic lesions. *Eye (Lond)*. 2009;23:497–503.
8. Biesemeier A, Schraermeyer U, Eibl O. Chemical composition of melanosomes, lipofuscin and melanolipofuscin granules of human RPE tissues. *Exp Eye Res*. 2011;93:29–39.
9. Katz ML, Gao CL, Rice LM. Formation of lipofuscin-like fluorophores by reaction of retinal with photoreceptor outer segments and liposomes. *Mech Ageing Dev*. 1996;92:159–174.
10. Sparrow JR, Dowling JE, Bok D. Understanding RPE lipofuscin. *Invest Ophthalmol Vis Sci*. 2013;54:8325–8326.
11. Warburton S, Davis WE, Southwick K, et al. Proteomic and phototoxic characterization of melanolipofuscin: correlation to disease and model for its origin. *Mol Vis*. 2007;13:318–329.
12. Armstrong D, Koppang N, Nilsson SE. Canine hereditary ceroid lipofuscinosis. *Eur Neurol*. 1982;21:147–156.

13. Burke TR, Duncker T, Woods RL, et al. Quantitative fundus autofluorescence in recessive Stargardt disease. *Invest Ophthalmol Vis Sci.* 2014;55:2841–2852.
14. Delori FC, Dorey CK, Staurenghi G, et al. In vivo fluorescence of the ocular fundus exhibits retinal pigment epithelium lipofuscin characteristics. *Invest Ophthalmol Vis Sci.* 1995;36:718–729.
15. Holz FG, Schutt F, Kopitz J, et al. Inhibition of lysosomal degradative functions in RPE cells by a retinoid component of lipofuscin. *Invest Ophthalmol Vis Sci.* 1999;40:737–743.
16. Kelly JP, Weiss AH, Rowell G, Seigel GM. Autofluorescence and infrared retinal imaging in patients and obligate carriers with neuronal ceroid lipofuscinosis. *Ophthalmic Genet.* 2009;30:190–198.
17. Radu RA, Yuan Q, Hu J, et al. Accelerated accumulation of lipofuscin pigments in the RPE of a mouse model for abca4-mediated retinal dystrophies following vitamin a supplementation. *Invest Ophthalmol Vis Sci.* 2008;49:3821–3829.
18. Font RL, Zimmerman LE, Armaly MF. The nature of the orange pigment over a choroidal melanoma. Histochemical and electron microscopical observations. *Arch Ophthalmol.* 1974;91:359–362.
19. Lavinsky D, Belfort RN, Navajas E, et al. Fundus autofluorescence of choroidal nevus and melanoma. *Br J Ophthalmol.* 2007;91:1299–1302.
20. Grossniklaus HE, Kivela T, Harbour JW, Finger P. Protocol for the examination of specimens from patients with uveal melanoma - protocol applies to malignant melanoma of the uvea. - College of American Pathologists Cancer Protocols, 7th ed. 2013.
21. McDowell EM, Trump BF. Histologic fixatives suitable for diagnostic light and electron microscopy. *Arch Pathol Lab Med.* 1976;100:405–414.
22. Spurr AR. A low-viscosity epoxy resin embedding medium for electron microscopy. *J Ultrastruct Res.* 1969;26:31–43.
23. Riechardt AI, Gundlach E, Joussem AM, Wilderding GD. The development of orange pigment overlying choroidal metastasis. *Ocular Oncol Pathol.* 2015;1:93–97.
24. Damato BE, Foulds WS. Tumour-associated retinal pigment epitheliopathy. *Eye (Lond).* 1990;4(Pt 2):382–387.
25. Hashmi F, Rojanaporn D, Kaliki S, Shields CL. Orange pigment sediment overlying small choroidal melanoma. *Arch Ophthalmol.* 2012;130:937–939.
26. Elner SG, Elner VM, Nielsen JC, et al. Cd68 Antigen expression by human retinal pigment epithelial cells. *Exp Eye Res.* 1992;55:21–28.
27. Fuchs U, Kivela T, Tarkkanen A. Cytoskeleton in normal and reactive human retinal pigment epithelial cells. *Invest Ophthalmol Vis Sci.* 1991;32:3178–3186.